DEVELOPMENT AND EVALUATION OF A BIOFIDELIC SHOULDER FOR THE IHRA (JARI) PEDESTRIAN MODEL

Michael S Neale
Brian J Hardy
Graham J L Lawrence
TRL Limited
United Kingdom

Paper 05-0096

ABSTRACT

Alterations were made to the shoulders of the Japan Automobile Research Institute (JARI) pedestrian model. The International Harmonised Research Activities Pedestrian Safety Group (IHRA PSG) has chosen the JARI pedestrian model as a basis to develop an improved humanoid pedestrian model. It is anticipated that when the development and validation of this model has been finalised it can be used to refine the current IHRA pedestrian head impact test procedures. In the work described here the shoulders of the JARI pedestrian model were improved to more accurately represent the structure and range of movement observed in real shoulders. Improvements to the model were validated by comparing the original and modified models' predictions against measures from Post Mortem Human Surrogate (PMHS) shoulder impact studies presented in the published literature. In contrast to the original JARI model the predictions from the modified JARI model were comparable to equivalent measures from the PMHS impact studies. Predicted peak shoulder impact forces from the original JARI pedestrian model were up to eight times larger than those measured in the PMHS impact studies or predicted by the modified JARI pedestrian model. Vehicle to pedestrian impacts were then simulated with the original and modified JARI models and predicted head impact responses from the models were compared. Head impact velocities from the modified JARI model were between 0.33 and 1.43 m.s^{-1} (2 and 14 %) greater than those predicted by the original JARI pedestrian model. Furthermore, it was found that a vehicle strike to the rear of the pedestrian models rather than to the side, lead to an increase in head impact velocity of up to 4.55 m.s^{-1} (39 %). However, before the IHRA PSG make decisions on the JARI model's head impact predictions further reviews of its structure and biofidelic responses are needed.

INTRODUCTION

The International Harmonised Research Activities Pedestrian Safety Group (IHRA PSG) has developed a sub-system head impact test procedure for assessing the aggressiveness of vehicle fronts in pedestrian head impacts. Many details of the IHRA head impact test procedure have been provisionally based on the predictions from pedestrian models developed by the Japan Automobile Research Institute (JARI), the National Highway Traffic Safety Administration (NHTSA) in the US and the Road Accident Research Unit (now the Centre for Automotive Safety Research, CASR) in Australia. These three models are lumped-mass models developed and run in the MADYMO code. Under the same impact conditions it was found that the three pedestrian models predicted significantly different head impact conditions. Therefore, the working group decided to develop an improved humanoid pedestrian model. The JARI model was chosen as a basis for the improved model because they were willing to make it available to the working group members. The intention of the working group is to identify and refine all the body parts of the model important to producing biofidelic head impact conditions. When the development and validation of this model is considered satisfactory, then it can be used to refine the current head impact test methods.

It is anticipated that the response of the shoulder during vehicle to pedestrian impacts will be important to the resulting impact conditions for the head, especially if the shoulder strikes the bonnet first prior to the head impact. Previous work has been completed reviewing the shoulder response of the JARI pedestrian model under impact (Neale *et al*. 2003a,b) with a view to developing the model for the purpose of refining the IHRA pedestrian head impact test procedure. In comparison to measured results from PMHS shoulder impact studies presented in the published literature, it was found that the JARI pedestrian model provided a very poor representation of the human shoulder response under impact and was found to be very rigid. Furthermore, the modifications made to the modelled shoulders were not detailed enough to provide an acceptable representation of the biofidelic impact response of the human shoulder. For example, the shoulder to shoulder (acromion to acromion) displacement, predicted by Neale's 2003 modification to the shoulder of the JARI pedestrian model was less than 1 mm, compared with an average of 39 mm as measured in Post Mortem Human Surrogates (PMHS) under equivalent shoulder impact conditions. The shoulder response of a further pedestrian model developed by TNO was also reviewed by Neale in 2003, this version of the TNO model was also found to provide a very rigid shoulder response compared with the measures obtained from the PMHS shoulder impact studies.

However, TRL understand that the TNO shoulder has been improved since.

It is anticipated that a rigid shoulder, as is present in the JARI pedestrian model, could provide increased protection to the head in comparison to a real shoulder. This raises concerns on the accuracy of the model's predicted head impact conditions for the purpose of developing the IHRA head impact test procedures. Consequently, in response to this concern TRL Limited undertook a further study described here, funded by the UK Department for Transport (DfT), to develop a more biofidelic representation of the shoulder for the IHRA (JARI) pedestrian model.

THE JARI PEDESTRIAN MODEL

Figure 1 shows the external structure of the JARI pedestrian model. The model represents a 50th percentile male pedestrian with a mass of 72.5 kg. It consists of 27 anatomical segments joined by a series of kinematic joints. Table 1 details the connections between the anatomical segments of the model. With the exception of the elbows, the segments of the model are joined by a series of spherical or 'ball-and-socket' joints. The elbows are formed from revolute or 'hinge' joints. All the joints have a defined stiffness characteristic to approximate the stiffness and range of motion of the equivalent anatomical joint. In addition to the regular anatomical joints such as the knees and elbows, further joints have been implemented in the model to simulate the bending response of the long bones in the legs and arms. These have stiffness characteristics approximating the moments needed to bend the bones in these segments of the body. These joints are 8, 10, 13, 15, 18, 20, 23 and 25 in Table 1.

The JARI model was operated in this study with the bending response of the bones in the arms and neck locked (*i.e.* joints 5, 6, 18, 20, 23 and 25 in Table 1), and matched the model setup that had been used for runs of the model completed by the IHRA pedestrian working group (IHRA Pedestrian Safety Working Group, 2002).

MODIFICATIONS TO THE SHOULDER OF THE JARI PEDESTRIAN MODEL

The arms in the original JARI model are joined to the torso by spherical joints (joints 17 and 22 in Table 1) which are intended to characterise the complete relative range of movement between the torso and the upper part of the arm. In reality the connection between the torso and the upper arm consists of a much more complicated series of anatomical joints, ligaments, muscles and tendons connecting a series of bones in the shoulder. This more complex structure provides a more diverse range of movement in the shoulders compared with the spherical joints that have been used in the

original JARI model. For instance, as shown by Neale *et al.* (2003a,b) published results from shoulder impacts to PMHS reveal a considerable degree of relative movement between the shoulders when impacted (*i.e.* acromion-acromion displacement), but this same response could not be recreated in the original JARI pedestrian model.

Figure 1. The JARI pedestrian model.

Figure 2 details the osseous features of the human shoulder. At the anterior medial location of the shoulder the clavicle bone forms the sternoclavicular joint with the sternum, which is located at the centre of the rib cage. The lateral aspect of the clavicle forms the acromioclavicular joint with the acromion, a bony protrusion of the triangular shaped scapula bone, which lies on the posterior of the rib cage. The main body of the scapula bone is secured to the rib cage by a large number of back muscles. This configuration enables the scapula to freely float over the surface of the rib cage allowing a considerable amount of movement in the shoulder. Inferior to the acromioclavicular joint, the humerus (upper arm bone) connects with the scapula to form the humeroscapular joint.

Modifications made to improve the shoulder of the JARI pedestrian model aimed to recreate as close as possible the physical structure and movement of the real shoulder. Figure 3 provides schematics of the improved shoulder developed for the JARI pedestrian model. At the location of the pedestrian model's sternum a spherical joint overlays a planar joint which is rigidly fixed to the torso of the pedestrian model. The planar joint was introduced to consider the anticipated compression and displacement of the rib cage during shoulder

impacts, allowing a degree of medial-lateral and fore-aft movement only at this connection during simulated shoulder impacts. The spherical joint was introduced to represent the movement in the sternoclavicular joint. Axial rotation in this joint has been locked, although the joint is free to flex (rotate) in all other directions.

Table 1
Anatomical segments and joint connections of the JARI pedestrian model

Joint number	Joint description	Joint type	Joint initial condition
Spine and neck			
1	Pelvis-Lumbar	Spherical	Free
2	Lumbar-Abdomen	Spherical	Free
3	Abdomen-Thorax	Spherical	Free
4	Thorax-Clavicle	Spherical	Free
5	Clavicle-Neck	Spherical	Locked
6	Neck-Head	Spherical	Locked
Right and left legs			
7 & 12	Pelvis-Hip	Spherical	Free
8 & 13	Hip-Femur	Spherical	Free
9 & 14	Femur-Knee	Spherical	Free
10 & 15	Knee-Tibia	Spherical	Free
11 & 16	Tibia-Ankle	Spherical	Free
Right and left arms			
17 & 22	Clavicle-Shoulder	Spherical	Free
18 & 23	Shoulder-Upper arm	Spherical	Locked
19 & 24	Upper arm-Elbow	Revolute	Free
20 & 25	Elbow-Lower arm	Spherical	Locked
21 & 26	Lower arm-Hand	Spherical	Free

Connected to the spherical joint is a translational joint representing the bending response of the clavicle. The lateral aspect of the translational joint is connected to horizontal and diagonal Kelvin elements which are fixed at their opposite ends to the posterior aspect of the pedestrian model's torso. The connection between the translational joint and the Kelvin elements is intended to be equivalent to the acromioclavicular joint. The intention of the Kelvin elements is to represent the resistance of the scapula bone as it slides over the surface of the rib cage.

Further to the connection between the translational joint and the Kelvin elements a hinge joint has been overlaid to consider the anticipated relative rotation and movement of the scapula about the acromioclavicular joint. Inferior to the hinge joint a planar joint has been introduced to represent the relative give within the humeroscapular joint under impact. Fore-aft and superior-inferior movement occurs in this joint but no rotation. Overlaying this planar joint a spherical joint has been introduced matching the type and stiffness characteristics of the joints used in the original JARI model to represent the complete shoulder response (*i.e.* joints 17 and 22 in Table 1). This spherical joint in the modified JARI pedestrian model is intended to represent the free range of motion typically observed in the humeroscapular joint.
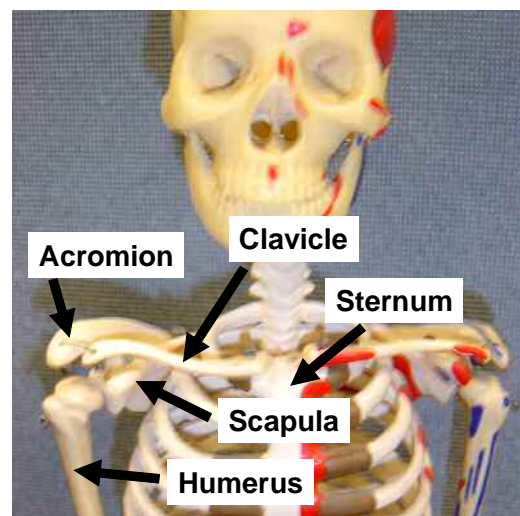
Anterior view of the shoulder
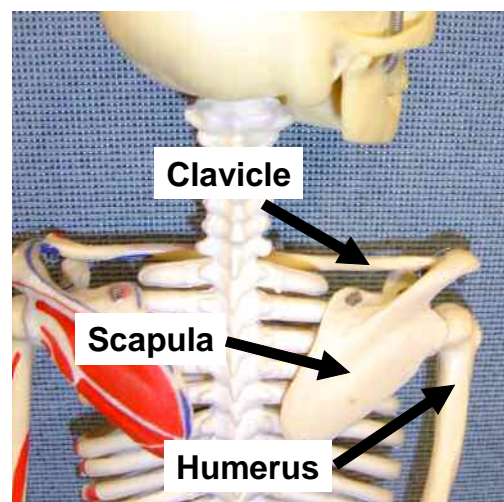
Posterior view of the shoulder

Figure 2. Details of the human shoulder.

The location of the spherical joints representing the humeroscapular joints were maintained in the same positions as joints 17 and 22 (see Table 1) in the original JARI model. The position of the remaining joints used in the construction of the improved shoulders for the JARI pedestrian model

were based on measures presented in the published literature (Robbins, 1983).

Anterior view of shoulder model

Plan view of shoulder model
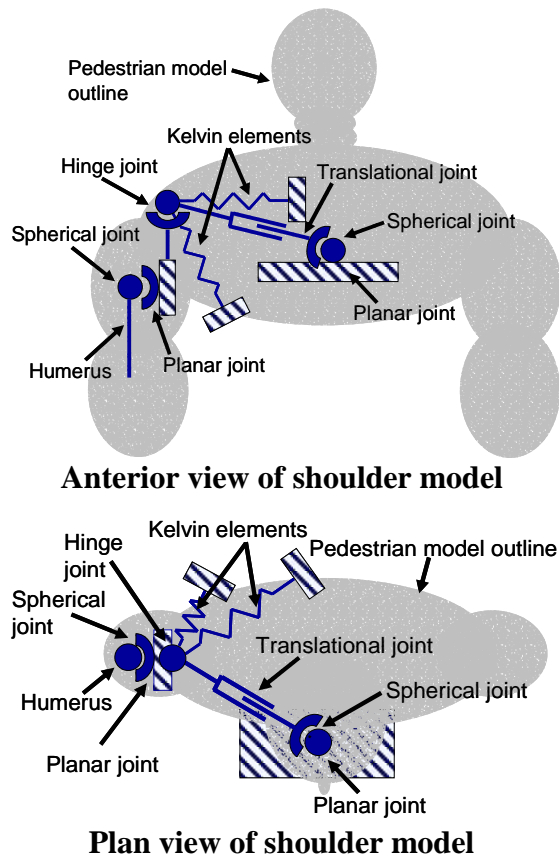
Figure 3. Schematic of the modifications made to the shoulder of the JARI pedestrian model.

EVALUATION OF THE MODIFIED JARI MODEL'S SHOULDER RESPONSE

The stiffness characteristics and range of movement in the shoulder structures of the modified JARI pedestrian model were tuned to approximate comparable measures from the Post Mortem Human Surrogate (PMHS) shoulder impacts studies of Compigne *et al.* (2003). In these impact studies four fresh PMHS were used as detailed in Table 2. For the impacts the PMHS were seated on a bench and instrumented with tri-axial accelerometers secured at the following anatomical locations:

- In the mid-sagittal plane at T1 and sternum locations.
- To both the left and right hand sides of the internal and external clavicle extremities and into both acromion.
- On the impacted side only, two were screwed to the medial and inferior angles and two were screwed laterally onto the humerus, approximately 100 and 250 mm below the head of the humerus.

The PMHS were struck by a guided impactor weighing 23.4 kg and fitted with a rigid

150 x 80 mm rectangular impacting plate. A load cell was placed behind the impacting plate in order to record the impact force on the shoulder. The recorded force was corrected by a factor of 1.066 to allow for the mass of the impacting plate placed in front of the load cell.

Table 2
Details of the PMHS used in the shoulder impact studies of Compigne *et al.* (2003)

Subject	Age (yrs)	Sex	Weight (kg)	Height (cm)	Shoulder width (mm)	Shoulder flesh thickness (mm)	
						Left	Right
1	77	F	67	161	335	20	24
2	88	M	33	163	355	10	12
3	79	F	52	159	355	12	10
4	82	F	50	155	345	15	15

The right shoulder of each PMHS was subjected to three sub-injurious impacts in which the initial impactor velocity was approximately 1.5 m.s^{-1}. For the three repeated shoulder impacts the PMHS were rotated at 0, +15 and -15 degrees with respect to the impact ram, as shown in Figure 4. Following the three sub-injurious impacts to the right shoulder the PMHS were subjected to a 0 degrees injurious impact to the left shoulder. For two of the PMHS the initial velocity of the impactor for the injurious impacts was approximately 4.2 m.s^{-1} and for the remaining two PMHS the left shoulders were impacted by an impactor having an initial velocity of approximately 6.0 m.s^{-1}.

The original and modified versions of the JARI pedestrian model were modified to match the set-up of the various shoulder impact tests as shown in Figure 5. Limited details were available concerning the set-up of the PMHS's for the tests and many of these were estimated in the models. These included details on the exact seating posture of the PMHS and the geometry and structure of the bench that the PMHS were seated on for the impact tests. The simulated contact friction between the pedestrian models and the simulated bench was set at 0.3.

As noted above, repeated shoulder impact simulations were completed with the modified JARI model and the joint characteristics and range of motion in the joints of the modified JARI shoulder were altered in order to tune the response of the model to that of the PMHS test data. During these simulations it was also found necessary to make the following additional alterations to the setup of the modified JARI pedestrian model:

- It was found during simulated shoulder impacts with the modified JARI pedestrian model that the contact definition between the high upper arm ellipsoids and the upper thorax ellipsoid (Figure 5) was obstructing the

relative shoulder to shoulder displacement. It was rationalised that this contact definition placed an unrealistic constraint on the model as the relative displacement between the shoulders will be mainly controlled by the anatomical connections between the shoulders. As such, the contact definition between the high upper arm ellipsoids and the upper thorax ellipsoid was removed.

- During simulated shoulder impacts with the modified JARI pedestrian model it was found that the contact definition between the high lower arm ellipsoids and the lower thorax ellipsoid (Figure 5) was obstructing the relative shoulder to shoulder displacement. It was rationalised that the offending contact definition was too stiff and did not allow for the fact that the thorax ellipsoids provide a poor representation of the stiffness and profile of the real human thorax. Hence, this contact definition was altered to allow approximately 4 cm of free penetration between the ellipsoids in the contact prior to a contact restoring force being activated.

- The contact stiffness of the high upper arm ellipsoids (Figure 5) in the modified JARI pedestrian model was reduced. This lead to a slightly softer contact between the impactor and the right shoulder of the modified JARI pedestrian model in comparison to that generated between the impactor and the right shoulder of the original JARI pedestrian model. This change in the stiffness for the contact definition was partly based on the measured shoulder skin thickness of PMHS made by Compigne *et al*. (2003) as shown in Table 2. The contact stiffness of the high upper arm ellipsoids was also changed from a non-elastic contact to an elastic contact.
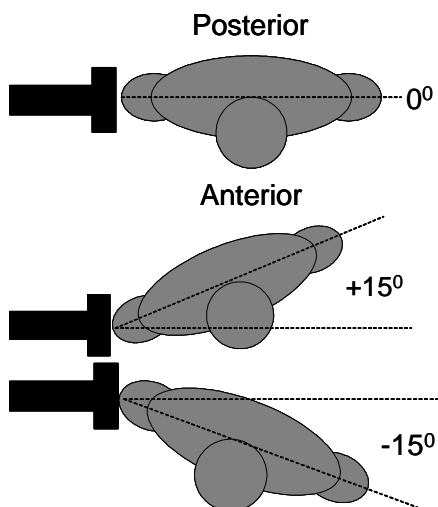
Figure 4. Setup of the PMHS sub-injurious right shoulder impacts from Compigne *et al.* (2003).

In addition to these modifications the mass of the original and modified JARI pedestrian models was reduced from 72.5 kg to 50.5 kg, equalling the average mass of the PMHS used in the impact tests. This was achieved by scaling the mass of each anatomical component of the modified and original JARI models by 0.69.
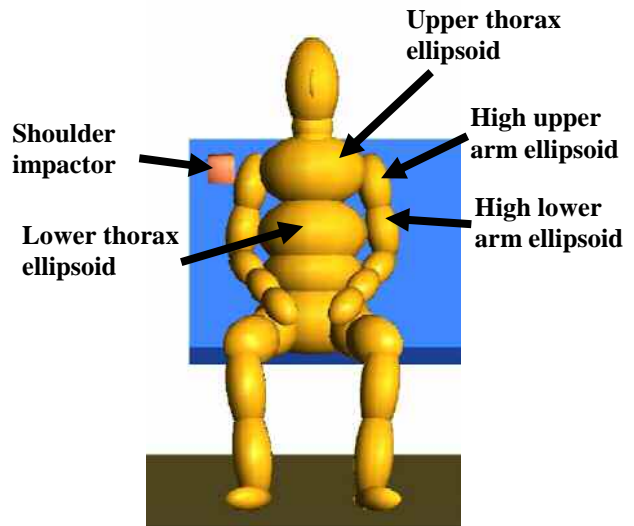
Figure 5. Set-up of the JARI pedestrian model for the simulated shoulder impacts.

Results - Evaluation of the modified JARI model's shoulder response

The versions of JARI pedestrian model developed and applied in this study were run under the version 6.1 release of MADYMO. Furthermore, all experimental and simulated predictions were filtered at CFC180. For the evaluation the impact forces and acromion to acromion deflections predicted by the original and modified JARI pedestrian models were compared against equivalent measures made in the PMHS shoulder impact tests of Compigne *et al.* (2003).

Sub-injurious shoulder impact conditions - Measured and predicted shoulder impact forces and acromion to acromion displacements measured in the PMHS shoulder impact tests and predicted by the modified JARI pedestrian model are presented in Figure 6. As shown in the figure the predicted results are comparable in both magnitude and duration to those measured, for all directions in which the sub-injurious impacts to the right shoulders of the PMHS were simulated. In contrast to these results Figure 7 includes the predicted shoulder impact force from the original JARI pedestrian model for the 0° shoulder impact. It is noticeable in these results that the peak predicted shoulder impact force from the original JARI pedestrian model are over three times greater than those measured and predicted by the modified JARI pedestrian model. Furthermore, the profile of

the shoulder impact response is very different from that measured and predicted by the modified JARI pedestrian model. In the instance of the shoulder impact force there is an initial peak in predicted shoulder impact force followed by a series of short pulses due to a "chattering" contact between impactor and shoulder. This is a consequence of having a completely inelastic contact definition between the impactor and the shoulder in the original JARI pedestrian model. As described above this has been changed to an elastic contact definition for the modified JARI pedestrian model.

It has been shown by Neale *et al.* (2003a,b) that the shoulders of the original JARI pedestrian model are rigidly connected and do not displace with respect to each other under shoulder impacts, *i.e.* zero acromion to acromion displacement under all impact conditions. This behaviour is considerably different from that measured in the PMHS and predicted by the modified JARI pedestrian model, as shown in Figure 6, where even for the sub-injurious impacts the peak acromion to acromion displacement is between 5 and 25 mm.

Impactor to shoulder contact force   **Acromion to acromion displacement**

0° Shoulder impact

+15° Shoulder impact
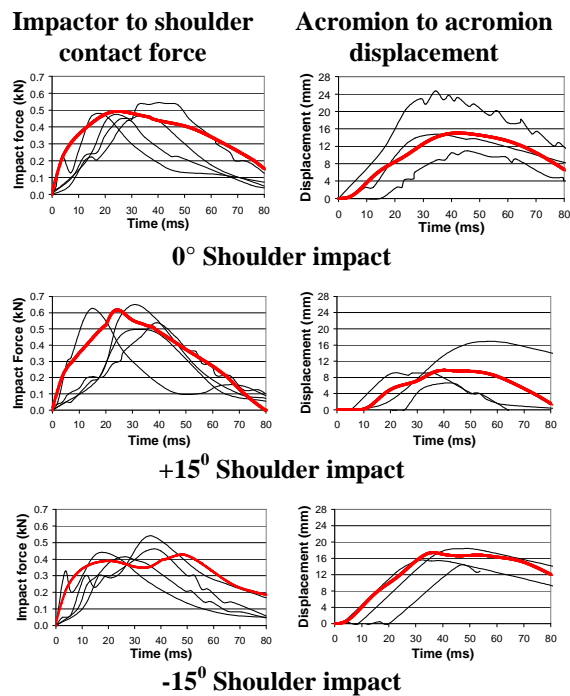
-15° Shoulder impact

Figure 6. **Comparison of the modified JARI model's predictions (red) with measured results from the PMHS sub-injurious impact tests of Compigne *et al.* (2003) (black).**

Injurious shoulder impact conditions - For the injurious shoulder impact conditions the modified JARI model again provides comparable predictions of shoulder impact force and acromion to acromion displacement to those measured, as shown in Figure 8. A noticeable difference in the results is that the modified JARI model predicts a second larger peak in shoulder impact force which

is not observed in the experimental results. It is anticipated that this may be due to the fact that the modified model is currently unable to simulate damage to bones and ligaments of the shoulder. This explanation and behaviour is consistent with the lower peak values of acromion to acromion displacement predicted by the modified JARI model compared with those measured in the PMHS tests.
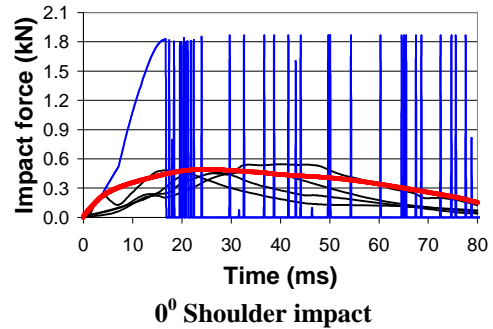
0⁰ Shoulder impact

Figure 7. **Comparison of the original JARI model's predicted shoulder impact force (blue) with that predicted by the modified JARI model (red) and measured in the PMHS sub-injurious impact tests of Compigne *et al.* (2003) (black).**

Impactor to shoulder contact force   **Acromion to acromion displacement**

4.2 m.s⁻¹ Shoulder impact velocity

6.0 m.s⁻¹ Shoulder impact velocity
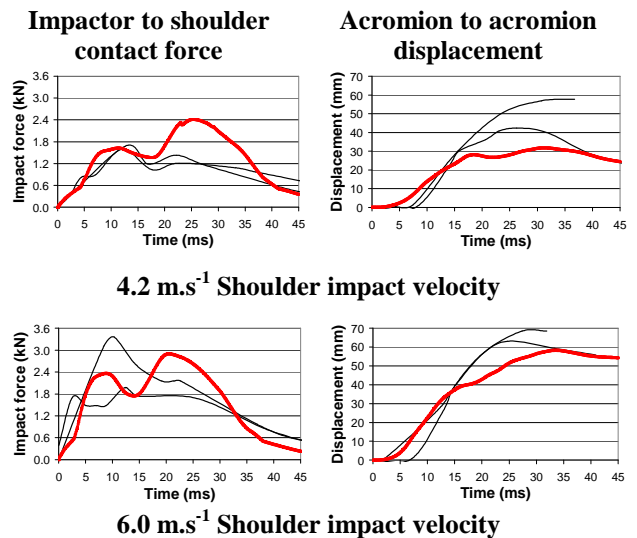
Figure 8. **Comparison of the modified JARI model's predictions (red) with measured results from the PMHS injurious impact tests of Compigne *et al.* (2003) (black).**

Figure 9 overlays the predicted shoulder impact forces from the original JARI pedestrian model with those measured in the PMHS tests and predicted by the modified JARI pedestrian model for the injurious shoulder impacts. The peak predicted shoulder impact forces from the original JARI pedestrian model are over eight times larger than those measured and predicted by the modified JARI pedestrian model and exhibit the same "chattering" response as predicted for the sub-

injurious impact conditions. As previously noted, the original JARI model does not simulate acromion to acromion displacement.
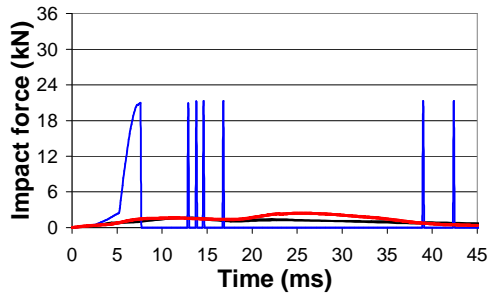
Impactor velocity = 4.2 m.s⁻¹
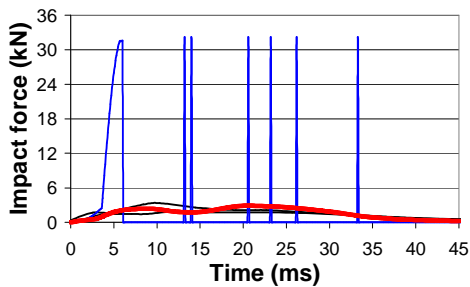
Impactor velocity = 6.0 m.s⁻¹

Figure 9. Comparison of the original JARI model's predicted shoulder impact force (blue) with that predicted by the modified JARI model (red) and measured in the PMHS injurious impact tests of Compigne *et al*. (2003) (black).

COMPARISON OF VEHICLE TO PEDESTRIAN HEAD IMPACT RESPONSES

Five simulated pedestrian to vehicle impacts were completed with the original and modified versions of the JARI pedestrian model in order to assess the influence that the changes to the shoulder of the model have had on its predicted head impact response. Details of the setup of the simulations are presented in Table 3. Three vehicle shapes and two initial vehicle speeds were used in the simulations. The pedestrian models for the simulations were set in a natural walking posture as shown Figure 10, which closely matched the WP2 stance set for the pedestrian models in the simulated pedestrian impacts completed by the IHRA and detailed in the IHRA Pedestrian Safety Working Group paper (2002). In all the simulations the pedestrian models were struck on the right hand side by the simulated vehicle, with the exception of model setup 5 in Table 3 in which the pedestrian models were rotated by 90° and were struck from the rear, as shown in Figure 11. These additional runs were completed to consider an impact condition in which the shoulder does not strike the bonnet and would not influence the interaction of the head with the vehicle.

The structure of the simulated vehicle in the model runs matched that used by the IHRA in their model runs, as shown in Figure 11. It is constructed from three cylinders defining the edges of the bumper, bonnet and lower limit of the vehicle front. Planes have been joined between these cylinders to form the skart, bumper, bonnet and windscreen of the simulated vehicle. These geometric shapes were repositioned and resized to obtain the desired vehicle shapes for the simulated vehicle to pedestrian impacts. As indicated in Table 3 the pedestrian impact with the Mid-sedan at 40 km.h⁻¹ was repeated with a long and short bonnet to consider impacts in which the head respectively hits the bonnet and windscreen of the vehicle. The stiffness characteristics for the structures of the simulated vehicle were chosen to provide a "safe" vehicle impact with the pedestrian, with the bonnet, bumper and bonnet leading edge of the simulated vehicle having a maximum contact load of 4 kN past 0.02 m of contact penetration, as shown in Figure 12. The simulated friction between the soles of the feet and ground was set at 0.67 and that between the pedestrian dummy and the vehicle front was set at 0.3. For all the impacts the simulated vehicles had a simulated braking acceleration of 0.5 g.

Front   Side
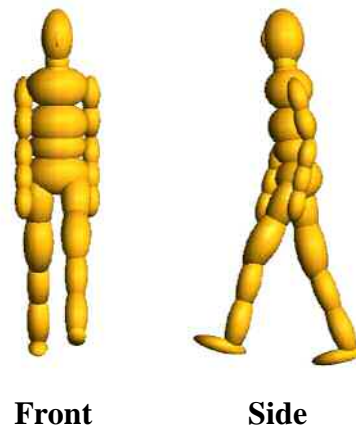
Figure 10. Posture of the JARI pedestrian models for the simulated vehicle to pedestrian impacts.

Results – Comparison of head impact conditions

Table 4 provides the predicted head impact conditions and head, shoulder and neck loads from the original and modified JARI models' predictions for the simulated vehicle to pedestrian impacts. Also included in the table are predictions from comparable simulated vehicle to pedestrian impacts completed by the IHRA working group with the original JARI pedestrian model (shaded values). However, in the simulations completed by the IHRA the arms of the pedestrian model were folded in front of the torso and the contact stiffness of the principle front end vehicle structures was

200 kN/m, *i.e.* considerably greater than the stiffness of the modelled vehicle used in the present study. Both of these vehicle stiffnesses are shown in Figure 12. The additional results from the IHRA provide added understanding on the variability that can be expected in the predictions from the model depending on how the simulations are set up.

Side impact of JARI model

Rear impact of JARI model
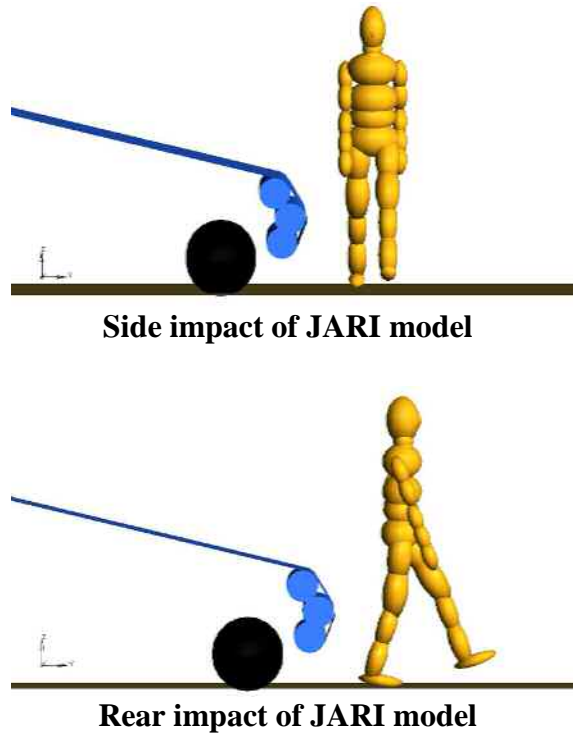
Figure 11. Orientation of the JARI pedestrian models for the simulated vehicle to pedestrian impacts.

Included in Table 4 are the effective head impact masses from the model runs which were calculated according to the following formula:

$$m = \frac{\int_{t_1}^{t_2} F\,dt}{\Delta v} = \frac{\int_{t_1}^{t_2} F\,dt}{\int_{t_1}^{t_2} a\,dt}$$

A discussion on the different methods available for calculating effective mass can be found in Annex A.

Direct comparisons of the original and modified JARI model predictions obtained in this present study (*i.e.* all values in Table 4 excluding those that are shaded) provides an indication of the influence that the modifications to the shoulder have had on the model's predictions. For these comparisons it is shown in Table 4 that the modified JARI pedestrian model predicts resultant head impact velocities which are between 0.33 to 1.43 m.s^{-1} (2 to 14 %) greater than those predicted by the original JARI pedestrian model. Overall, neither of the models consistently predicts the greatest head impact

angles, although differences in these predictions range between 0.01 and 11.8° (0.01 and 32 %).
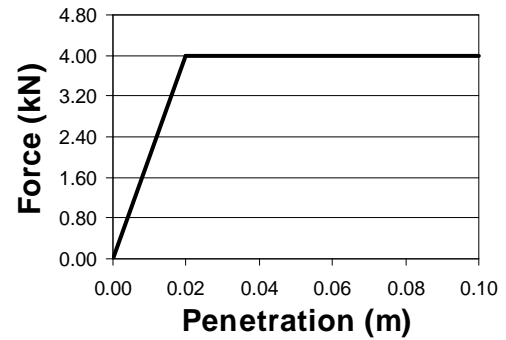
(a)
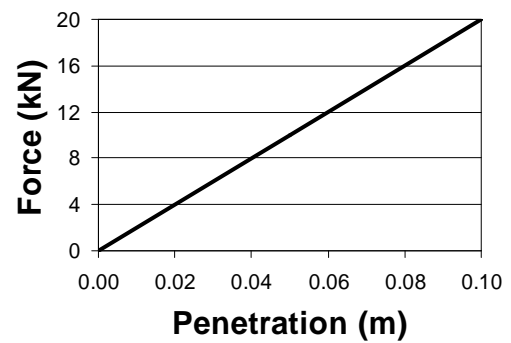
(b)

Figure 12. Stiffness characteristics of the modelled vehicle – (a) as used in the present study (pedestrian friendly vehicle characteristics) and (b) as used in the JARI model runs completed by the IHRA.

A comparison of the predicted head impact velocities for setups 2 and 5 shows that rotating the pedestrian model by 90[0] so that it is struck from the rear leads to an increase in the head impact velocity of 3.45 (28 %) and 4.55 m.s^{-1} (39 %) for the modified and original models respectively.

Predicted head impact forces were almost consistently the same at 4.18 kN, which was consistent with the upper contact load limit of 4 kN set for the bonnet in the model runs as shown in Figure 12. Similarly, none of the predicted shoulder impact forces exceeded 4.18 kN. An exception to this trend was the head impact force predictions from model setup 1 which exceed 5 kN as a result of the modified and original JARI model heads striking the simulated windscreen, which had stiffer contact characteristics than the bonnet. In all the simulations completed the impact was sufficient to cause an acromion to acromion displacement greater than 30 mm in the modified JARI pedestrian model.

Table 3
Setup of the simulated vehicle to pedestrian impacts completed with the original and modified versions of the JARI pedestrian model

Model setup	Vehicle	Model stance	Vehicle speed (km.h^{-1})	Bonnet length
1	Mid-sedan	Mid-stance	40	Short
2	Mid-sedan	Mid-stance	40	Long
3	Mid-sedan	Mid-stance	30	Long
4	Mid-SUV	Mid-stance	40	Long
5	Mid-sedan	90^0 Rotated stance	40	Long

Table 4
Comparison of the modified and original (in brackets) JARI model predictions for simulated vehicle to pedestrian impacts. Shaded values are comparable values obtained by IHRA in their model runs of the original JARI pedestrian models with pedestrian unfriendly vehicle contact forces

	Model setup (see Table 3)				
	1	**2**	**3**	**4**	**5**
Resultant head impact velocity (m.s^{-1})	12.05 (11.39) 9.0	10.75 (9.32) 9.0	9.46 (9.01) 10.91	12.08 (10.93)	14.20 (13.87)
Ratio of head impact and vehicle velocity	1.08 (1.02) 0.81	0.97 (0.84) 0.81	1.13 (1.08) 1.31	1.09 (0.93)	1.28 (1.25)
Head impact angle (°)	43.46 (44.91) 60.1	80.82 (69.05) 78.4	84.58 (81.65) 44.0	84.84 (84.83)	29.47 (40.49)
Effective head impact mass (kg)	5.12 (4.34)	4.23 (4.13)	4.21 (4.02)	3.63 (3.60)	6.12 (4.98)
Head impact force (kN)	5.66 (5.20)	4.18 (4.18)	4.18 (4.18)	4.18 (4.18)	4.18 (4.18)
Head to neck force (kN)	3.8 (3.4)	4.4 (2.6)	3.10 (3.06)	3.9 (3.0)	3.9 (4.66)
Acromion to acromion displacement (mm)	48.2 (0.0)	42.0 (0.0)	34.0 (0.0)	50.0 (0.0)	44.1 (0.0)
Shoulder impact force (kN)	3.60 (3.83)	4.18 (4.18)	3.07 (4.18)	3.16 (4.18)	3.78 (4.18)

Differences in the resultant head impact velocities and head impact angles predicted by the modified JARI pedestrian model with those previously obtained by the IHRA (shaded values in Table 4) range between 3.0 m.s^{-1} (29 %) and 40.6° (63 %) respectively. In two out of three of the possible comparisons of the results in Table 4 the resultant head impact velocities predicted by the modified JARI pedestrian model are greater than those previously obtained by the IHRA and in

model run 3 the predicted head impact velocity from the JARI pedestrian model is lower than that previously obtained by the IHRA. Unfortunately it is not possible to interpret the reasons for this outcome on account of the fact that in addition to the shoulder structure the posture of the pedestrian model and stiffness of the vehicle structure was different for these two sets of model runs. As such, it is not possible to gauge which of these differences has contributed to this shift in the pattern of the results. However, the comparison of these model predictions does highlight the variations that can be obtained in the predictions from the JARI model compared with those that have previously been obtained by the IHRA and used in the development of the IHRA sub-system head impact test procedures.

DISCUSSION

The modifications made to the JARI pedestrian model in this work have improved considerably the biofidelic impact response of the model's shoulders. These modifications have also had a considerable influence on the predicted head impact response of the JARI model's head during simulated vehicle to pedestrian impacts. This confirms the anticipated understanding at the onset of the work that the shoulder response is important to the dynamic response of the head during vehicle to pedestrian impacts.

Strictly speaking the biomechanical evaluation does not show that the modified shoulder validates as inputs to the model have been altered (iteratively) in order to get the model's predictions to match PMHS shoulder impact test results. These adjustments were made primarily to the characteristics of the Kelvin elements introduced into the shoulder, while fixed estimates were made for the characteristics of the joints added to the model. This was necessary because the required biomechanical data, which would typically be obtained from sub-system testing of the shoulder structure, was not available and certain anatomical features which would influence the shoulder response were not explicitly modelled. Nevertheless, by matching the key physical structures of the shoulder in the model with those of a real human and obtaining good agreement in five different impact conditions for the same model setup it is considered that the biofidelic response of the improved shoulder has been robustly tested.

The results of this work have significant implications on the IHRA's use of the JARI pedestrian model for developing aspects of the IHRA pedestrian head impact test procedures. It is implied from the model's predictions that if the modified JARI pedestrian model developed in this study were adopted by IHRA then recommended initial head impact velocities for the IHRA sub-system test procedures would be higher than if the

original JARI pedestrian model was used to obtain test parameters for the test procedures. In view of the fact that the modified JARI pedestrian model has been shown to provide accurate predictions of PMHS shoulder impact results there is increased confidence that the modified JARI pedestrian model provides predicted head impact conditions that are more representative than those of the original JARI pedestrian model. However, no firm conclusions can be drawn on what the final ratio of head impact velocity to vehicle speed should be at this stage. This will only emerge once the IHRA working group have completed their task of identifying and refining all the body parts of the model important to producing biofidelic head impact conditions. When the development and validation of this model is considered satisfactory, then it can be used to refine the current head impact test methods. Therefore, it is recommended that the TRL modifications made to the shoulder of the JARI pedestrian model should be adopted by the IHRA Pedestrian Safety Working Group as a first step towards developing their improved biofidelic pedestrian model.

The previous modelling work completed on the JARI pedestrian model (Neale *et al.*, 2003a,b) attempted to improve the model's shoulder response by adopting the same shoulder structure as that used in the pedestrian model developed by CASR in Australia. In addition to this modification, further changes made to the structure of the model in this work included the removal of a secondary contact defined between the legs and arms of the model which was inadvertently introduced by the original authors of the model and the introduction of joints to simulate axial stretching in the spine, the details of which were also taken from the CASR pedestrian model. Despite the fact that the changes made to the shoulders of the model in this previous work did little to improve the biofidelic shoulder response of the model, in several vehicle to pedestrian impacts simulated with the modified and original JARI pedestrian models the modified pedestrian model provided predictions of head impact velocity between 0.33 and 0.86 m.s^{-1} (3.4 and 6.5 %) greater than those predicted by the original JARI pedestrian model. The suggestion is that there exist additional representative changes that could be made to the JARI pedestrian model in order to improve the accuracy of its predicted head impact response during vehicle to pedestrian impacts. For instance, it is known that the modelled JARI spine has a far simpler structure and response than that of a real human spine. It is most likely that this simplification of a spine would have a considerable influence on the impact response of the head during vehicle to pedestrian impacts.

It is noticeable from the models' predictions in this present study that the largest influence on the predicted head impact response arose by striking the model from the rear rather than from the side. It is important to note that the whole body kinematics of the JARI model have not been validated for rear impacts as it has been for lateral vehicle to pedestrian impacts (IHRA pedestrian safety working group, 2002). As such it is necessary to place some caution on the absolute accuracy of the rear vehicle to pedestrian impact predictions and the interpretations that can be made. However, it is anticipated from these predictions that in addition to improving the biofidelic response of the pedestrian model, there are further alterations that could be made to the setup of the accident situation (including pedestrian stance) which could have a greater influence on predicted head impact responses.

The current study used stiffness characteristics for the vehicle that were "safe", with a maximum load per contact of 4.0 kN (see Figure 12). This was done because the IHRA test procedures are likely to be used to type approve cars, in which case the stiffness of those real cars would have to be broadly similar to that used. The contact stiffness is likely to be one of the main factors contributing to the differences noted between the 'original JARI model' runs performed for this study by TRL and previously obtained by the IHRA. It is therefore preferable that models used to obtain test parameters for type approval tests should have an appropriate *i.e.* "safe" vehicle stiffness, so that the headform test is representative of a real head impact into a type-approved vehicle.

CONCLUSIONS

The aim of this investigation was to improve the shoulder response of the JARI pedestrian model, which has been chosen by the IHRA to develop the IHRA pedestrian sub-system head impact test procedure. The purpose of completing the work has been to improve the shoulder interaction of the pedestrian model during simulated vehicle to pedestrian impacts and so improve the resulting interaction of the head with the simulated bonnet. The modifications made to the shoulder of the pedestrian model have attempted to accurately represent the structure and range of motion of the anatomical shoulder. Overall, the conclusions of the work are as follows:

- An improved shoulder model has been developed for the JARI pedestrian model.
- In comparison to the original shoulder, the structure of the improved shoulder model provides a much closer structural representation of the real human shoulder anatomy.
- In comparison to the original shoulder model, predictions from the improved shoulder model closely match measured

responses from PMHS shoulder impact test results.

- In general, it is implied from the models' predictions that predicted head impact velocities for simulated vehicle to pedestrian impacts are higher for the JARI model with the improved shoulder model than they are for the original JARI pedestrian model. As such, the recommended IHRA sub-system head impact test velocities would be higher if the structure of the test method were based on the predictions from the JARI model with the improved shoulder response. However, no firm conclusions can be drawn on the correct head impact conditions until all body parts of the model, important to producing biofidelic head impact conditions, have been identified and improved.
- Although it is likely that the shoulder model could be further improved the robust testing of its biofidelic response suggests that it is sufficiently well developed for use by IHRA.
- It is thought likely that the other areas of the pedestrian model such as the spine may need to be improved before its predictions are sufficiently accurate for them to be used by IHRA to specify head impact conditions.

ACKNOWLEDGEMENTS

REFERENCES

Compigne S, Caire Y, Quesnel T and Verriest J (2003). *Lateral and oblique impact loading of the human shoulder 3D acceleration and force-deflection data.* IRCOBI Conference. Lisbon, Portugal, September 2003.

IHRA Pedestrian Safety Working Group (2002). *International Harmonized Research Activities Pedestrian Safety Working Group. 2002 report.* Document IHRA/PS/215 (1/2). Tokyo, Japan: Japan Automobile Standards Internationalization Center. (Document available at http://www-ihra.nhtsa.dot.gov/)

Neale M S, Hardy B J and Lawrence G J L (2003a). *Development and review of the IHRA (JARI) and TNO pedestrian models.* Proceedings of the 18th International Technical Conference on the Enhanced Safety of Vehicles (ESV), Nagoya, Japan, 19-22 May 2003.

Neale M S, Hardy B J and Lawrence G J L (2003b). *Development and review of the IHRA (JARI) and TNO pedestrian models.* TRL Project Report PR/SE/653/03.

Robbins D H (1983). *Anthropometric specification for mid-sized male dummy, Volume 2.* The University of Michigan, Transport Research Institute Report UMTRI-83-53-2. 2901 Baxter Road, Ann Arbor, Michigan 48109: University of Michigan.

ANNEX A: EFFECTIVE MASS CALCULATION FOR TRL HEADFORM PARAMETER MODEL

There are a number of ways of calculating effective mass when deriving a value for an impactor's mass. There are three decisions to be made:

- Use energy, impulse or average effective mass?
- Which direction to take?
- Which start and stop times to take when integrating?

Document IHRA PS215 (2002) has the formula

$$m = \frac{\int_{t_1}^{t_2} F/a \, dt}{(t_2 - t_1)}$$

. This is simply averaging the instantaneous effective mass values over the period t_1 to t_2. TRL hasn't used this method because it's possible to get values of acceleration (a) that are very close to zero. These would at best have too much influence in the final result and could at worst give a result that was significantly high. This risk is much greater when a specific direction is used rather than resultants.

The energy method uses the deformation energy (obtained from integrating force by penetration) and the Δv (which is of course the time integral of

$$m = \frac{2 * \int F \, ds}{(\Delta v)^2}$$

acceleration), and the formula

. TRL has used this method in the past, for upper legform masses.

The impulse method uses impulse (obtained from integrating force by time) and the Δv, and the

$$m = \frac{\int_{t_1}^{t_2} F \, dt}{\Delta v} = \frac{\int_{t_1}^{t_2} F \, dt}{\int_{t_1}^{t_2} a \, dt}$$

formula

. This is effectively average force over average acceleration. This is the method used for the results reported.

The effective mass can be different in different directions. Physically, the forces required to cause a given acceleration will depend on the direction.

For instance, at the knee the effective mass would be least in the knee's normal direction of movement (within its normal range), greater for lateral knee bending and highest of all for axial leg movement. The headform parameter model is being used to find the appropriate parameters for a headform impact into a bonnet. Although the headform may hit the bonnet at an angle, the Δv will be nearly normal to the bonnet, with the headform velocity parallel to the bonnet being relatively unchanged. Therefore, TRL considers that the effective mass normal to the bonnet is the appropriate one to take, obtained by taking both bonnet-to-head force and head acceleration normal to the bonnet, ignoring orthogonal components. Using resultant acceleration would include neck interactions that cause head accelerations parallel to the bonnet, which are not appropriate for a headform impactor.

One pair of runs with the normal length bonnet involved head to windscreen impact; in this case the force and acceleration were taken normal to the windscreen.

IHRA PS215 (2002) gave three options for the start and stop times of the integration. The 10% effective mass method is unlikely to work if the forces and accelerations are taken normal to the bonnet, as the effective mass will be more constant over the time history. The dummy model HIC window can be quite different to the actual head to bonnet impact, because of acceleration components parallel to the bonnet, and hence to the eventual headform HIC window. TRL therefore prefers and has used the 10% force method.

IHRA PS215 (2002) doesn't specify what points are taken when the time histories are not uni-modal. Where this occurred the period taken was from the first to the last 10% force value. However, in other cases if there should be a brief spike it might be more appropriate to take only the main part.